Combined Effect of Shear and Nucleating Agent on the Multilayered Structure of Injection-Molded Bar of Isotactic Polypropylene

Jing Cao, Ke Wang, Wen Cao, Qin Zhang, RongNi Du, Qiang Fu

Department of Polymer Science and Materials, State Key Laboratory of Polymer Materials Engineering, Sichuan University, Chengdu 610065, People's Republic of China

Received 30 April 2008; accepted 1 October 2008
DOI 10.1002/app.29540
Published online 28 January 2009 in Wiley InterScience (www.interscience.wiley.com).

ABSTRACT: Molten polymers are usually exposed to varying levels of shear flow and temperature gradient in most processing operations. Many studies have revealed that the crystallization and morphology are significantly affected under shear. A so-called "skin-core" structure is usually formed in injection-molded semicrystalline polymers such as isotactic polypropylene (iPP) or polyethylene (PE). In addition, the presence of nucleating agent has great effect on the multilayered structure formed during injection molding. To further understand the morphological development in injection-molded products with nucleating agent, iPP with and without dibenzylidene sorbitol (DBS) were molded via both dynamic packing injection molding (DPIM) and conventional injection molding. The structure of these injection-molded bars was investigated layer by layer via SEM, DSC, and 2 days-WAXD. The results indicated that the addition of DBS had similar effect on the crystal size and its distribution as shear, although the later decreased the crystal size more obviously. The combination of shear and DBS lead to the formation of smaller spherulites with more uniform size distribution in the injection-molded bars of iPP. A high value of *c*-axis orientation degree in the whole range from the skin to the area near the core center was obtained in the samples molded via DPIM with or without DBS, while in samples obtained via conventional injection molding, the orientation degree decreased gradually from the skin to the core and the decreasing trend became more obvious as the concentration of DBS increased. © 2009 Wiley Periodicals, Inc. J Appl Polym Sci 112: 1104–1113, 2009

Key words: poly (propylene); shear; nucleation; injection molding

INTRODUCTION

In most polymer processing operations (e.g., extrusion, injection molding, spinning), molten polymers are usually exposed to varying levels of shear flow and temperature gradient. Many studies have been carried out to investigate molecular orientation and resultant morphology under different shear-flow conditions in laboratory. Shear-induced shish-kebab texture in semicrystalline polymers has attracted more and more attentions due to the significant theoretical values and potential in practical applications.[1–7] Although the shear flow in industrial processing is considered to be weak and may not be able to induce the extended molecular chain, many studies have revealed that the crystallization and morphology are significantly affected under shear flow in industrial processing.[8–13] It is found that a so-called "skin-core" structure is usually formed in injection molded semicrystalline polymers such as isotactic polypropylene (iPP) or polyethylene (PE). During the injection molding process, the hot polymer melt contacting with the cold walls of the mold experiences high shear stress, high strain and rapid cooling rate, resulting in a layer with high orientation near the wall to be the skin. However, in the remainder of the specimen there is a spherulitic structure called the core, caused by the lower shear stress and lower cooling rate, which lead to a relaxation of molecular chains. The model of the lamellar orientation morphology near the surface for injection-molded bar of iPP has been proposed in the literature,[14–17] in which it is suggested that there is a bi-model oriented structure of *c*-axis and *a**-axis orientation for crystallite generated in shear region. The c-axis orientation here is referred to the lamellae having their folding chains or c-axis preferentially aligned along the flow direction whereas the *a**-axis orientation referred to the lamellae having their

Correspondence to: Q. Fu (qiangfu@scu.edu.cn).
Contract grant sponsor: National Natural Science Foundation of China; contract grant numbers: 20404008, 50533050, 20490220.
Contract grant sponsor: Special Funds for Major State Basic Research Projects of China; contract grant number: 2003CB615600.

folding chains preferentially perpendicular to the flow direction.

The hierarchical structure formed in injection-molded product is predominately determined by molding conditions (e.g., molding temperature, injection speed, injection pressure, and cooling time etc.), chemical nature of certain polymers and molecular parameters (e.g., molecular weight, molecular weight distribution, chain branching, and molecular architecture). The presence of nucleating agent and other polymer components could also have a great effect on the multilayered structure formed during injection molding. The results of the experiments undertaken by Zhu et al.[18] showed that the degree of the overall orientation of injection-molded iPP was remarkably improved with the amount of nucleating agent (sodium benzoate, SB) increasing over a broader range of sample thickness, compared with those in the absence of SB. In other words, the lamellar orientation of injection-molded bar of iPP at a given depth was remarkably enhanced by the addition of SB. The phenomenon of SB-mediated inclination of oriented structure is interesting and the mechanism remains open for debate.

In our previous works, the dynamic packing injection molding (DPIM) technology, which relies on the application of shear stress fields to melt/solid interfaces during the packing stage by means of hydraulically actuated pistons, was introduced to prepare injection-molded bars. The main feature of DPIM is that after the melt is injected into the mold the specimen is forced to move repeatedly in the chamber by two pistons that move reversibly with the same frequency as the solidification progressively occurs from the wall to the molding core, resulting in a multilayered structure in the final specimen.[19] On the basis of the intensive investigations of the multilayered structures of the injection molded bar by DPIM,[20–22] some peculiar structures, such as, epitaxial growth between iPP and HDPE,[23] transcrystallization of iPP on glass fiber,[24] cocontinuous phase morphology of LLDPE and iPP blends,[22] have been achieved in the products of real processing.

It is interesting to find that a nucleating agent could not only increase the crystallization temperature and decrease the crystal size, but also improve the overall orientation of injection-molded iPP, as reported by Zhu et al. As introducing shear is also a common method to increase the crystallization temperature and improve the overall orientation of a polymeric material. One expects a combined effect on the crystal morphology and orientation of a polymer by introducing both nucleating agent and shear. In this work, the multilayered structures of injection molded bar of iPP containing dibenzylidene sorbitol (DBS), a kind of α-nucleating agent of iPP, were investigated in detail by means of 2D-WAXD, SEM and DSC. The samples were prepared via both dynamic packing injection molding and conventional injection molding. The objective of our work is twofold. The first is to further verify the effect of nucleating agent on the degree of orientation of injection molded bars along the sample thickness; the second is to investigate the combined effect of shear and nucleating agent on the multilayer structure of injection molded bar, for better control of the morphology and properties of injection-molded products.

EXPERIMENTAL

Materials

In this research, iPP was used as based polymer, and dibenzylidene sorbitol (DBS) was used as nucleating agent. A commercially available iPP (T30S) with a MFI of 2.0 g/10 min, measured at 190°C under 2.16 Kg loading, was purchased from Du Shanzi Petrol Company. The average weight molecular weight Mw and the average number molecular weight M_n are 3,99,000 and 86,740 g/mol, respectively. Thus, its molecular weight distribution is roughly 4.6. The nucleating agent DBS was kindly supplied by Nanjing Agent Factory.

Samples preparation

Nucleating agent was firstly mixed with iPP in a twin-screw extruder (TSSJ-25 corotating twin-screw extruder) at a concentration of 2.0 wt % to produce a masterbatch. The masterbatch was diluted to desired DBS concentrations, 0.1 and 0.5 wt %, by mixing with fitting amounts of pure iPP. In this article, pure iPP without DBS is named 0PP, and iPP with 0.1 and 0.5 wt % DBS is named 0.1PP and 0.5PP, respectively. The temperature of the extruder was maintained at 160, 190, 200, 200, and 195°C from hopper to die and the screw speed was set at 120 r/min. All samples were molded by dynamic packing injection molding (DPIM) technology using SZ100g injection molding machine. In this work, the melt temperature was 200°C, the mold temperature was about 20°C, the dynamic packing pressure was 35 MPa, and the moving frequency of pistons was 0.3 Hz. The detailed introduction and experiment procedure can be found in Ref. 19. The injection molding under static packing was also carried out by using the same processing parameters but without shearing, for the purpose of comparison. The specimen obtained by dynamic packing injection molding is called dynamic sample, with a prefix "d"; otherwise, that obtained by static pacing injection molding is called static one, with a prefix "s." For example, "d0.1PP" means this sample contains

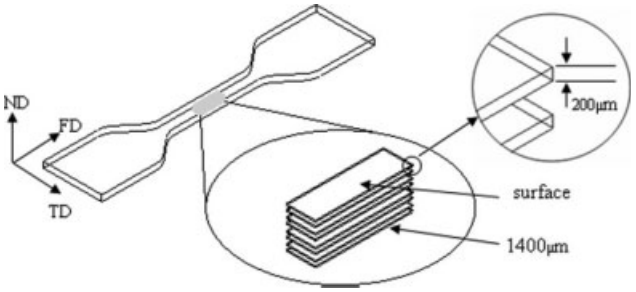

Figure 1 Schematic of the positions of the samples for 2D-WAXS and DSC measurement. FD, the flow direction; TD, the transverse direction; ND, the direction normal to the FD-TD plane.

0.1 wt % DBS and is obtained by dynamic packing injection molding.

Two-dimensional wide angel X-ray scattering

The distribution of orientated structure along the thickness direction was characterized by the two-dimension wide-angle x-ray diffraction (2D-WAXD). The testing samples were cut into pieces with a thickness of 200 μm from the surface to the core of molded bar at ND direction (as shown in Fig. 1). The 2D wide-angle x-ray scattering (2D-WAXS) experiments were conducted on a SEIFERT (DX-Mo8*0.4s) diffractometer equipped a 2D Mar345 CCD x-ray detector, operating at 40 kV and 30 mA. The wavelength of the monochromatic X-ray from Mo radiation was 0.71 nm and the sample-to-detector distance was 324 mm. The incident X-ray beam was set perpendicular to the flow direction. Azimuthal scans (0–360°) of 2D-WAXS were made for the corresponding lattice plane of iPP at a step of 1° to calculate the orientation fraction.

Scanning Electron Microscopy (SEM)

To check the lamellae structure, the specimen obtained was cryogenically fractured in the direction parallel to the flow direction in liquid nitrogen, and then etched by 1% solution of potassium permanganate in a mixture of sulfuric acid and 85% orthophosphoric acid to remove the amorphous phase.[25] After being cleaned by water, the etched surface was coated with gold and examined from the skin to the core layer by layer. The experiment was implemented on an X-650 Hitachi scanning electron microscope at 20 kV.

DSC measurements

The thermal analysis of the samples was conducted using a Perkin–Elmer Pyris-1 DSC, calibrated by indium. The DSC experiment was carried out in a nitrogen purged chamber. The slices were cut with a thickness of 200 μm from the surface to the core of both static and dynamic molded bars at a direction perpendicular to the molding direction-transverse direction plane, similar to the method used for the 2D-WAXD measurements (as shown in Fig. 1). Samples of weight 5 mg were cut from each slice for use in the DSC analysis. The sample was heated to desired temperature (200°C) at a rate of 10°C/min and held for a 5 min to eliminate the thermal history. Then the melt was cooled down to 50°C at 10°C/min.

RESULTS

Crystal morphology along sample thickness observed by SEM

Macroscopically, the main feature of injection-molded samples is the so-called skin-core morphology with tiny crystallites but oriented structure in the skin, and big spherulites but randomly orientated structure in the core. However, for the samples obtained via DPIM, more complicated skin-core structure is usually formed, and shear-induced morphologies with core, the oriented zone surrounding the core and the skin layer in the cross section areas

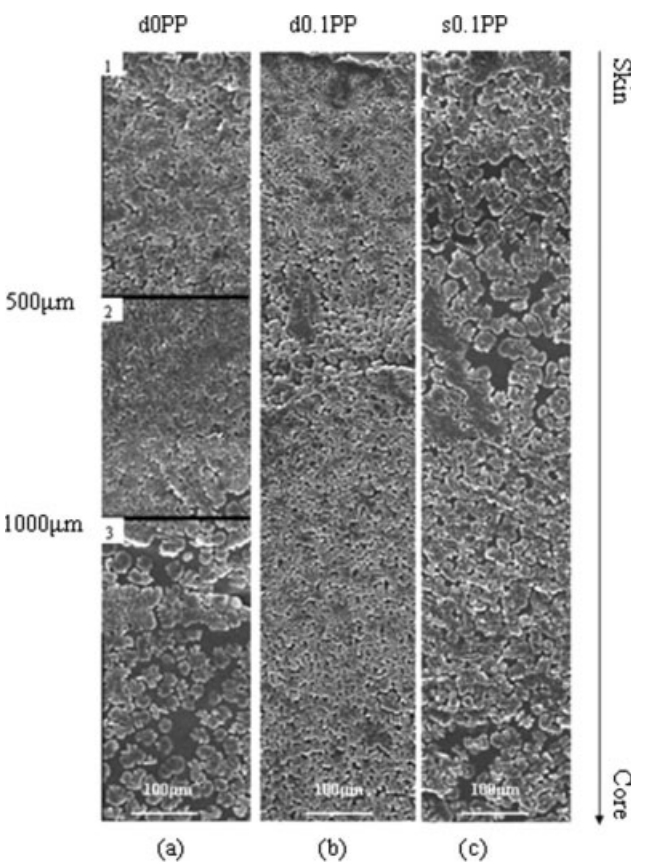

Figure 2 SEM microphotographs of etched sample of iPP with different concentration of DBS at magnification of 250 along the sample thickness: (a) d0PP; (b) d0.1PP; (c) s0.1PP.

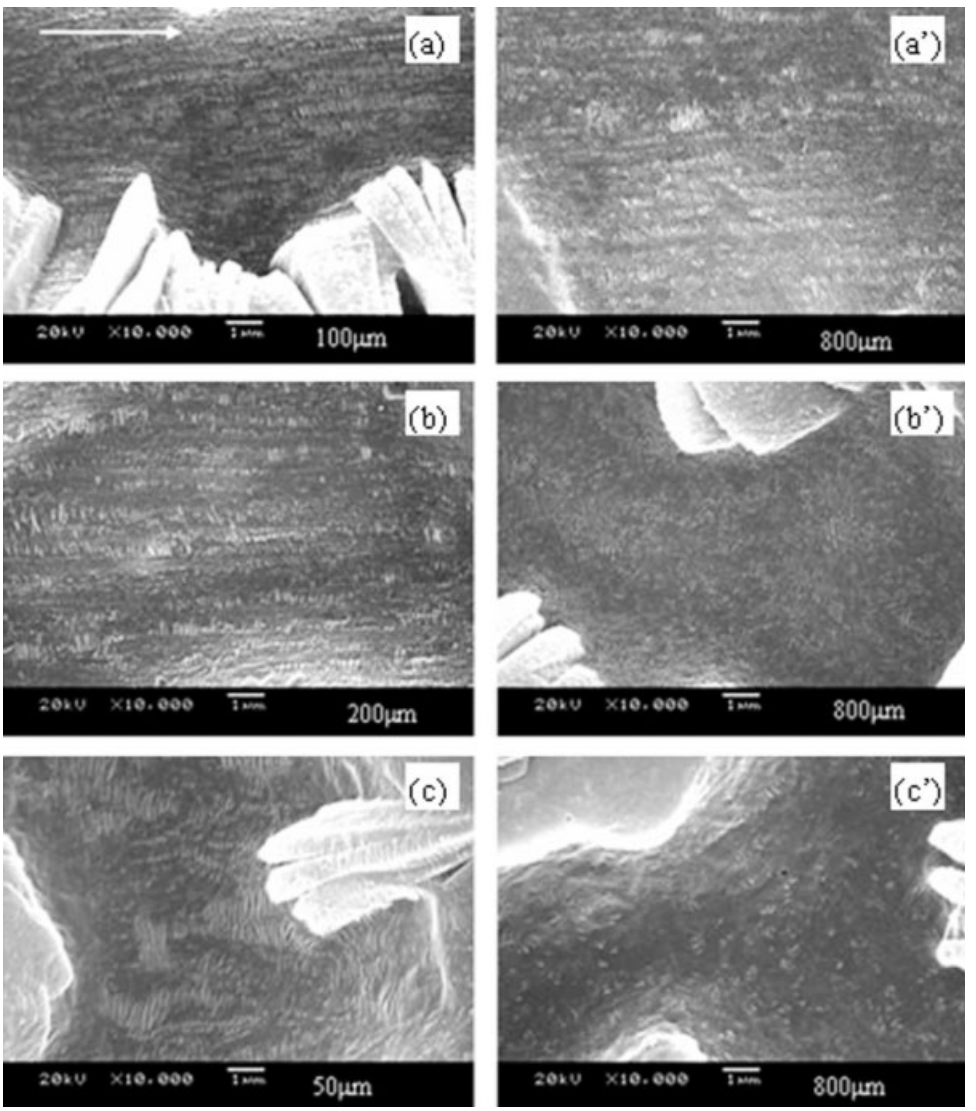

Figure 3 SEM microphotographs of etched samples at magnification of 10,000 along the sample thickness: (a) d0PP, at 100 μm; (a') d0PP, at 800 μm; (b) d0.1PP, at 200 μm; (b') d0.1PP, at 800 μm; (c) s0.1PP, at 50 μm; (c') s0.1PP, at 800 μm; arrow in schematic representing flow direction.

of the samples are often observed.[19,22] Figure 2(a) shows the development in size and distribution of the spherulites dispersed in the sample of d0PP from the skin to the core, as observed by SEM after etching. The SEM image could be divided into three parts: Region 1, from the most out surface to the layer with a depth of 500 μm from the surface; Region 2, the area with the depth from 500 to 1000 μm, and Region 3, from the layer with a depth of 1000 μm to the core. In Region 1 and 2, spherulite particles are densely dispersed in the matrix but the size of the ones formed in Region 1 is slightly larger than that in Region 2; in Region 3, the density of spherulites decreases and their size appears to be larger than that in Region 1 and 2. However, by adding nucleating agent DBS, no obvious skin-core morphology is observed along the whole sample thickness, as shown in Figure 2(b). One observes uniformly dispersed spherulite particles along the sample thickness, except of negligible change at the skin (0–200 μm) [Fig. 2(b)]. The suppression of skin-core morphology was reported in the literature by Li et al.,[26] who pointed out that the skin-core structure was suppressed due to a microfibrillar network formed in iPP/PET blends through shear controlled orientation in injection molding. For the sample s0.1PP, the size and distribution of spherulites are also uniform but with larger size, compared with its corresponding dynamic sample, as shown in Figure 2(c). So, it could be concluded that shear could result in a more complicated skin-core structure and adding nucleating agent will cause a uniform distribution of spherulite size along sample thickness, while the combination of shear and nucleating agent could lead to smaller spherulites with a more uniform size-distribution in the injection-molded bar of iPP.

A careful examination of the morphology underneath the observed spherulite at a higher magnification reveals more detailed structural characteristic of the injection-molded bars. As shown in Figure 3, for d0PP and d0.1PP, in addition to the spherulites, one observes the oriented lamellae aligned perpendicular to the shear flow direction, in both the skin area and the regions near core. For s0.1PP, however, the oriented lamellae are observed only in the skin region, and a random arrangement of lamellae is observed in the core region. So, the new finding is that the crystal morphology of the injection-molded bar of iPP is actually composed of two parts: the spherulites and the tiny lamellae. The diameter of spherulites is about 20-30 μm and the thickness of lamellae is less than 50 nm. The lamellae could be either oriented or randomly distributed, while the spherulites are composed of radially distributed lamellae. In general, final crystalline morphology such as large spherulite or small lamella is determined by molecular characteristics, nucleation rate, growth rate, duration of crystallization, solidification time, and son on. For all samples prepared in this study, static or dynamic and with or without nucleating agent, these two crystalline morphologies are observed, implying that external crystallization conditions and processing conditions should not be crucial for dominating type of crystalline morphology. We suggest that the formation of both the spherulites and the lamellae at given depth of the molded sample are probably caused from the broad distribution of iPP molecular weight. In the injection molding process, the melt temperature is 200°C, the temperature of mold wall is about 20°C and the sample thickness is 4.5 mm, thus an abrupt temperature gradient approximately 80°C/mm is expected at the very early moment after the melt is injected into the mold. On the other hand, the packing time is short, which is 3 min for the static samples and 5 min for the dynamic samples, indicating a short crystallization duration. Thus the size of spherulites and thickness of lamellar is quite dependent on the undercooling. In this case, the PP chains at the skin and core possess quite different undercooling degrees for crystallization. This effect could be dominant. On such a temperature gradient and crystallization time, the chains with high molecular weight hardly have enough time to crystallize into complete spherulites, they are most likely to form the tiny lamellae; whereas, the chains with lower molecular weight possess a high crystallization capability, they begin to crystallize at a higher temperature than the high M_w ones during the cooling process of solidification, thus have more chance to crystallize into big spherulites. A schematic depicting the crystal morphology including both spherulites and lamellae along the sample thickness of injection-molded bars is shown in Figure 4. It is notable that a preferential orientation of tiny lamellae with their *c*-axis parallel to the shear direction is found in the samples obtained via DPIM, while in the static samples, the tiny lamellae arrange randomly. This may be because the regular alignment of the shear-induced iPP chains along the flow direction could generate anisotropic crystalline precursors which serve as a template in the following crystallization and induce the oriented lamellar structure.

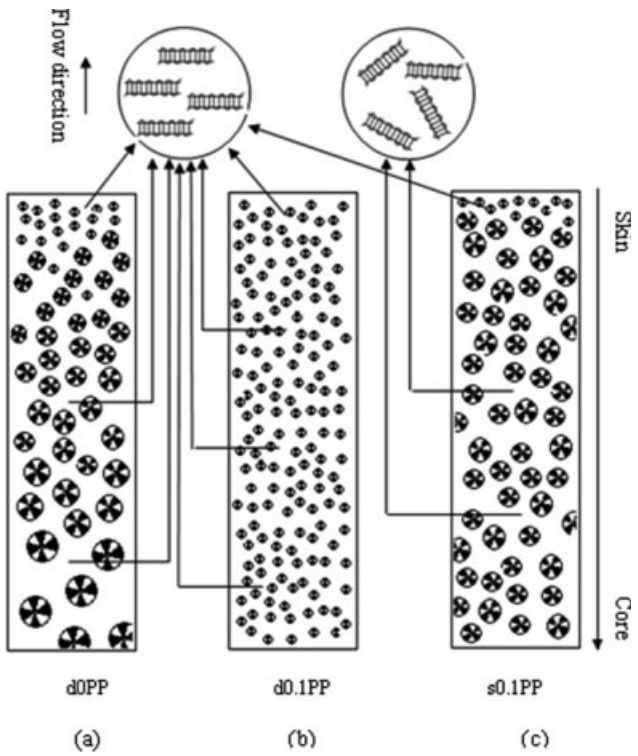

Figure 4 Schematic of crystal structure of iPP with different concentrations of DBS along the sample thickness: (a) d0PP; (b) d0.1PP; (c) s0.1PP.

The crystal structure as evidenced by DSC

The crystal structure and lamellae thickness in the injection-molded samples along the sample thickness can also be demonstrated by DSC experiment. Figure 5 shows the DSC heating curves of the specimens at each layer of both the static and dynamic injection-molded bars. One observes only one melting peak of α-crystal at 165°C throughout the whole region of each sample except the specimen near the skin which shows an additional weak peak at 145°C corresponding to the melting of β-crystal. The results of DSC heating thermograms show that only a small discrimination exists among the melting temperatures of all samples from the skin to the core, which is about 2°C, irrespective of the effect of nucleating agent and shear. It is observed that the melting peak of β-crystal shown in dynamic sample of iPP at 200 μm disappears at the same position as DBS is added.

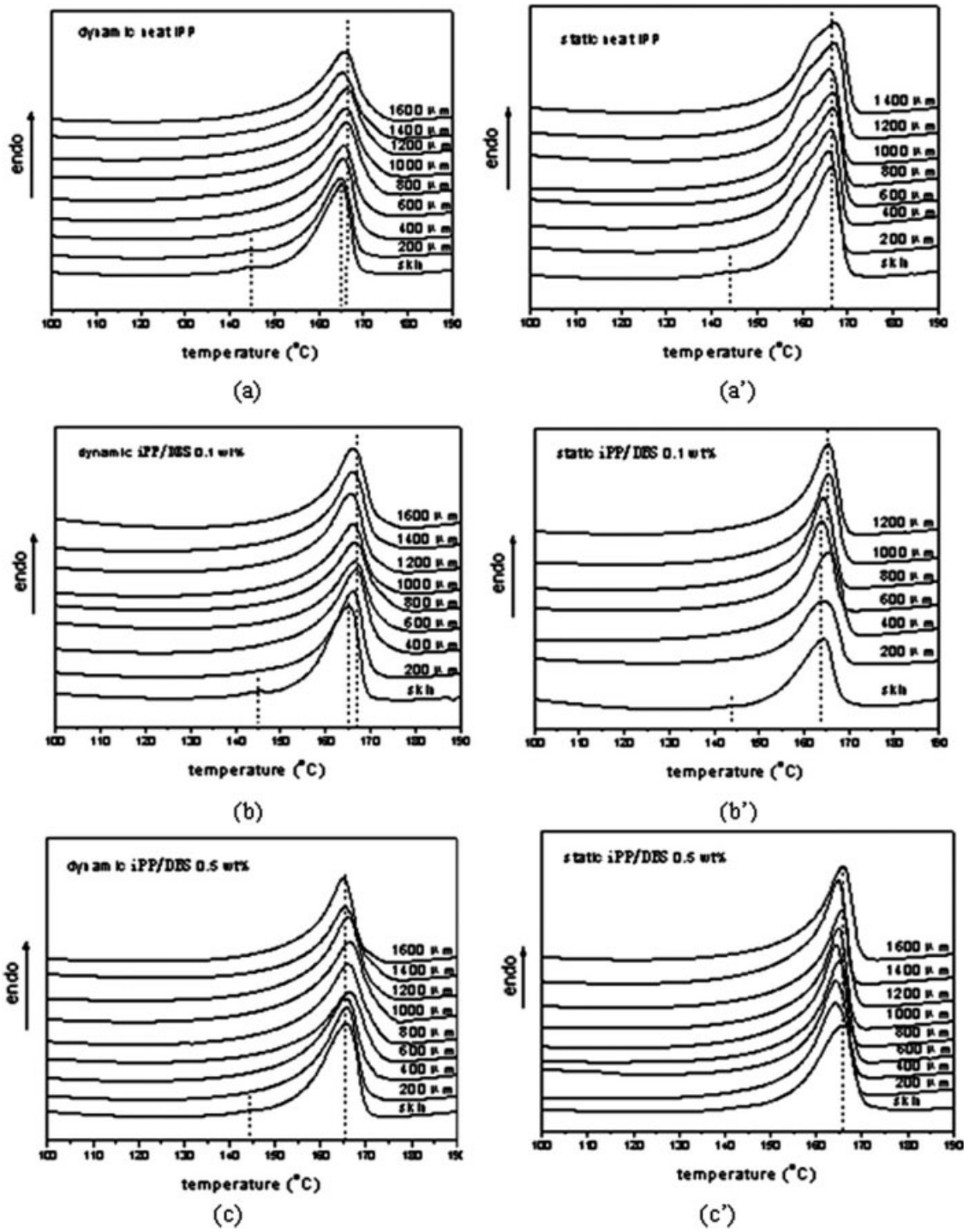

Figure 5 DSC heating curves at each layer of iPP containing different concentration of DBS for both dynamic and static samples: (a) d0PP; (a′) s0PP; (b) d0.1PP; (b′) s0.1PP; (c) d0.5PP; (c′) s0.5PP.

And, the intensity of the β-crystal at skin area decreases as the concentration of DBS increases for both dynamic and static samples. It is acknowledged that the position and the width of the peak in DSC curve represent the lamellae thickness and its distribution, respectively. By introducing shear, an obvious decrease of the peak width is observed for d0PP as compared with the static one [comparing Fig. 5(a) and Fig. 5(a′)], suggesting a shear-induced narrower distribution of lamellae thickness along sample thickness. This uniform lamellae thickness distribution can also be caused by the addition of DBS [comparing Fig. 5(a) and Fig. 5(b′)]. This result indicates that shear and DBS have a similar effect on the crystallization behaviors of iPP. The combined effect of shear and DBS on the DSC melting behavior

of injection-molded bar is not so obvious compared with that by only adding DBS or using shear [comparing Fig. 5(b) and Fig. 5(b′), or comparing Figure 5(b) and Figure 5(a′)]. Also the increase of DBS content has no obvious influence on the DSC melting behavior of iPP [comparing Fig. 5(c) and Fig. 5(b)]. It should be noted that although both big spherulites and tiny lamellae are observed via SEM for all the injection molded samples, DSC heating experiment could not distinguish the melting behaviors of these two kinds of crystal morphologies. Moreover, for the melting profiles of α-crystal in d0PP, as shown in Figure 5(a′), a shoulder is appreciable before the main melting peak, indicating the existence of lamellae with different thickness. Again this may be attributed to the molecular polydispersity which induces very different crystallization ability of polymer chains with different M_w; in addition, the gradient of crystallization temperature and the rearrangement of crystals during the DSC heating scans may also be responsible. However, imposing shear or adding nucleating agent can facilitate the crystallization by supplying large numbers of nuclei quickly at the early stage of crystallization, thus adjusting the crystallization kinetics of different chains to a similar level and inducing the formation of numerous spherulites and a relatively uniform distribution of lamellar thickness. As such the shoulder disappears in all dynamic samples and the static samples with nucleating agent, as shown in Figure 5 except (a′).

Shear-induced orientation detected via2D-WAXD

Figures 6 and 7 show the 2D-WAXD patterns of all dynamic and static samples at each layer. A series of obvious discrete reflections appear over the diffuse halo, which can be indexed as the (110), (040), (130), (111), and (−131) of the monoclinic α-form of iPP.[27,28] There is evidence of an additional reflection at the equator, whose 2θ is before and adjacent to the (040) plane of α-crystal, indicating the presence of β-crystal (300) in skin area of all dynamic and static sample. The result is exactly consistent with the DSC measurement (as shown in Fig. 5). As is known, the hk0 reflections represent lattice planes parallel to the *c*-axis, which in our experiments is in accordance with the flow direction. Consequently, the (040) intensity distribution around the equator indicates the expected crystallite orientation in the flow direction. The arcing in the meridian for (110) reflection and the spot intense in the equator for (110) and (040) reflection indicate that all dynamic samples studied exhibit some degree of orientation in each layer; however, the crystallite orientation for static samples is only observed in the skin area. The degree of orientation can be estimated quantitatively

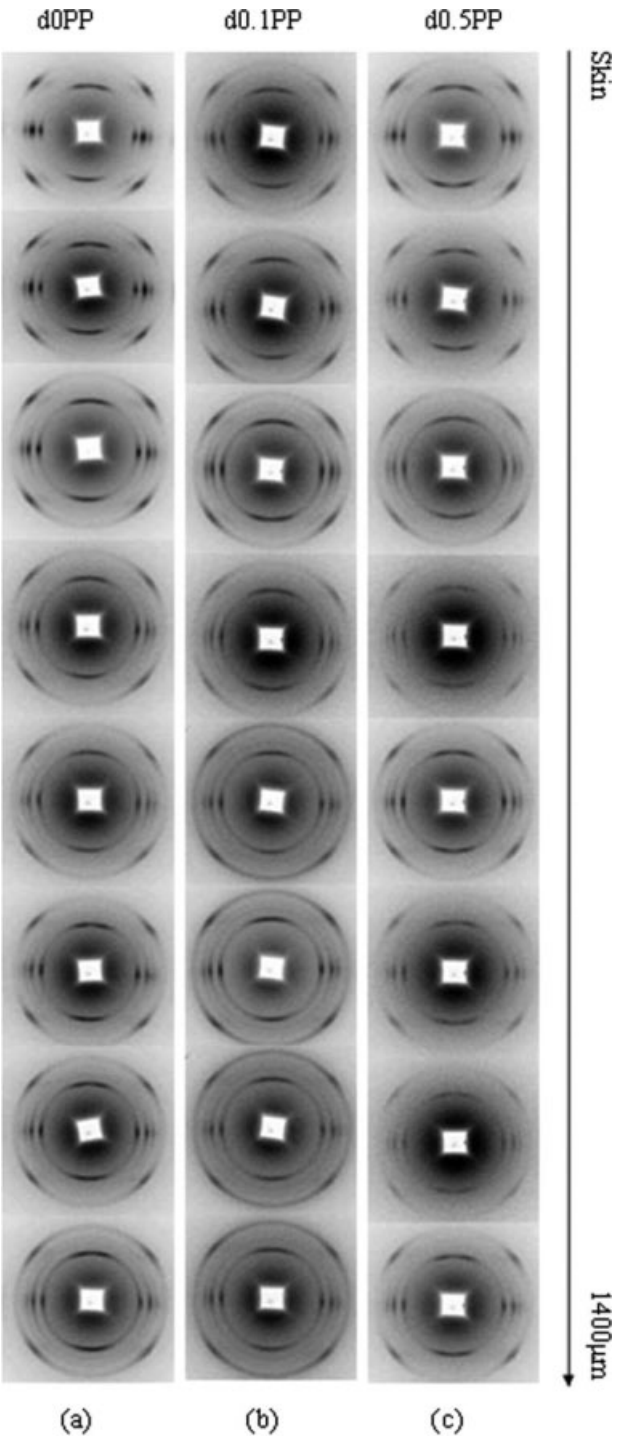

Figure 6 2D-WAXS patterns of dynamic sample of iPP with different concentration of DBS along the sample thickness, the arrow in left represent the flow direction: (a) d0PP; (b) d0.1PP; (c) d0.5PP (for each image, the shear flow direction is vertical).

by using the Hermans orientation function defined as follows:

$$f_H(\cos\varphi) = \frac{3\langle\cos^2\varphi\rangle - 1}{2}, \quad (1)$$

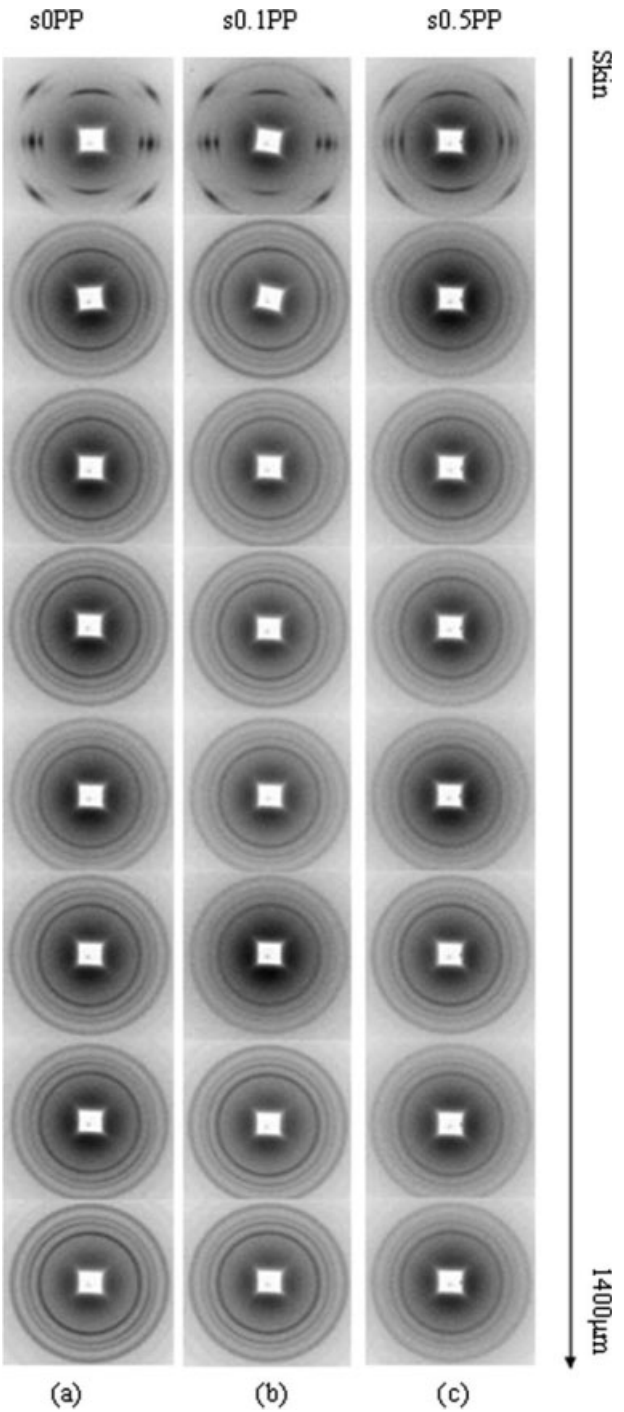

Figure 7 2D-WAXS patterns of static sample of iPP with different concentration of DBS along the same thickness, the arrow in left represent the flow direction: (a) d0PP; (b) s0.1PP; (c) s0.5PP (for each image, the shear flow direction is vertical).

where $\langle \cos^2 \varphi \rangle$ is an orientation factor defined as:

$$\langle \cos^2 \varphi \rangle = \frac{\int_0^{\frac{\pi}{2}} I(\varphi) \cos^2 \varphi \sin \varphi \, d\varphi}{\int_0^{\frac{\pi}{2}} I(\varphi) \sin \varphi \, d\varphi}, \quad (2)$$

where φ is an angle between the unit within a crystal of interest (e.g., c-axis) and a reference direction

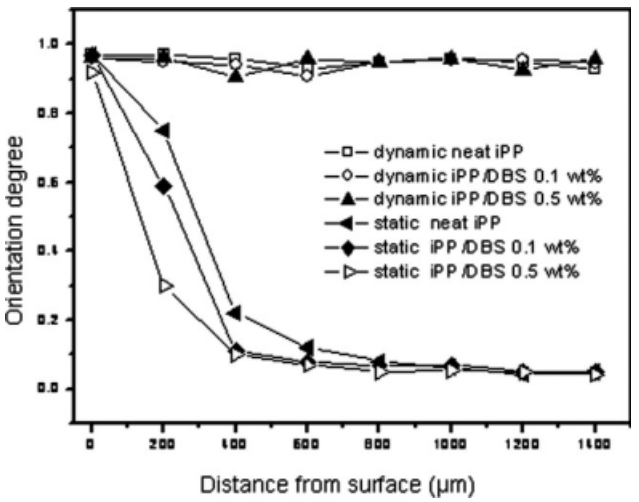

Figure 8 The c-axis orientation degree of dynamic and static sample of iPP containing different concentration of DBS at each layer calculated from α(040) intensity distribution along the azimuthal angle.

(flow direction in this work). And $I(\varphi)$ is the scattering intensity at φ. As is known, the (040) reflection corresponding to c-axis-oriented component is concentrated on the equator. According to that, the c-axis orientation degree of dynamic sample at each layer is calculated from the (040) intensity distribution along the azimuthal angle as shown in Figure 8. The orientation degree of d0PP is around 0.95 at each layer, and there is no evident change for the dynamic samples with DBS. For the static samples, the c-axis orientation in skin area is strong, while in the range of 400–1600 μm the orientation is so weak that nearly random orientation is detected. In addition, no obvious difference is observed among samples with different concentration of DBS. However, for the layer with a depth of 200 μm, the orientation degree decreases sharply as DBS is added into iPP ($f_H = 0.76$ for s0PP, $f_H = 0.58$ for s0.1PP, $f_H = 0.30$ for s0.5PP).

DISCUSSION

The effect of nucleating agent and shear stress on crystallization behavior and morphology

For conventional injection molding (static samples), DBS have strong effect on crystallization behavior and resultant crystal structure, such as, decreasing lamellar thickness and achieving uniform distribution of lamellar dimension in matrix, which are certainly due to the strong nucleation effect of DBS on the iPP crystallization. The results of DSC measurement have proven that DBS is a kind of outstanding nucleating agent since the crystallization temperature (T_c) of iPP can be significantly improved at a very low concentration of nucleating agent (0.1 wt %). Figure 9 shows DSC cooling thermograms of 0PP,

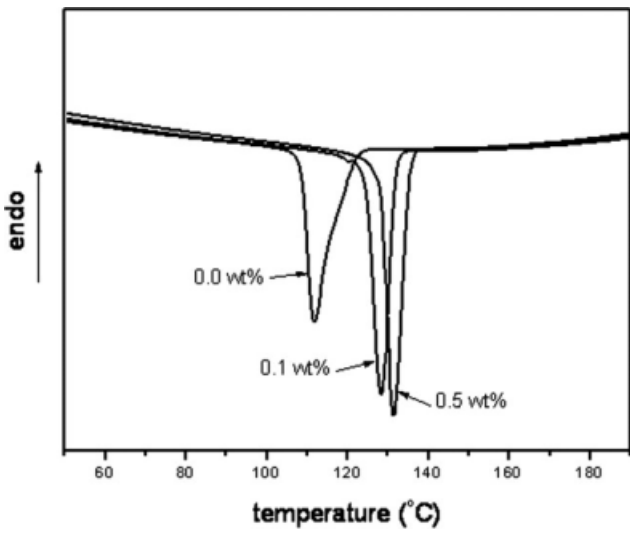

Figure 9 DSC cooling curves of iPP with different concentration of DBS.

0.1PP and 0.5PP samples from 200°C to 50°C at 10°C/min after holding at 200°C for 2 min. For a general expectation, adding nucleating agent into iPP will significantly increase the crystallization temperature by inducing numbers of nuclei in the primary nucleation process and as a result, form smaller spherulites and tiny lamellae. This can be proven by Figure 9, in which the crystallization temperature T_c, obtained from the minimum of exothermic crystallization peak is about 112°C for 0PP, When only 0.1 wt % DBS was added into iPP, there is a marked shift of crystallization peak toward a higher temperature, $T_c = 128$°C. Compared with the sample 0.1PP, T_c of the 0.5PP sample is slightly increased to 132°C. The data of enthalpy listed in Table I from which the crystallinity could be calculated, indicate that the crystallinity of iPP is improved by the addition of DBS.

As mentioned above, the feature of DPIM is to imply a continuous reversible shear force provided by periodically moving hydraulically actuated pistons after the melt being injected into the chamber until the solidification gradually occurs from the wall to the core part. So that the highly oriented structure along the shear flow direction can be seen in dynamic samples compared with the random distributed lamellae in static samples (as shown in Fig. 4), just as the 2D-WAXD patterns and SEM images revealed. Although the lamellar thickness of the samples obtained via DPIM seems not to be affected by the introduction of nucleating agent according to the DSC results (as shown in Fig. 5), a slight discrepancy of the size of spherulites and its distribution is directly observed by SEM (Fig. 2). It is reported that the flow field can increase crystallization rate and induce smaller crystal than that crystallized in quiescent condition, which is similar to the effect of nucleating agent. As shown in Figure 4, compared with sample s0.1PP, sample d0PP possesses smaller spherulites dispersed in the matrix. The result reveals that shear flow can decrease the crystal dimension more effectively compared with the addition of DBS. Furthermore, the combined effect of shear flow and nucleating agent can further decrease the size of spherulite.

The effect of nucleating agent and shear force on orientated structure

The main effect of shear is to assist the formation of nuclei by the alignment of polymer chains in the supercooled melt along the shear direction. These aligned chains may act as precursor for the formation of stable primary nuclei. Many primary nuclei can rapidly grow and forge connectivity along the flow direction to imprint the stress field. The growth of primary nuclei can be maintained or reinforced by a self-induced orientation of the molecules in front of the growing tip. The research explored by Shinichi et al.[29] suggested that the nucleation of bundle nucleus in isotropic or oriented melt in the presence of nucleating agent or dust particles is much easier than that without nucleating agent or dust particles under the same condition based on kinetic study, which induces the higher level of molecular or lamellar orientation. However, in this work, the consistent shear rate and strong shear stress due to the same frequency of moving piston and structural parameters of mold lead to very small variation of orientation degree ($f_H = 0.90$–0.97) in the region with a depth of 0–1400 μm for dynamic samples, irrespective of the addition of DBS. In this case, shear plays a dominant role in accelerating the crystallization and as a result, each layer from the skin to the core has almost the same degree of orientation. For the static samples, the value of orientation degree decreases with the depth and/or the amount of DBS increasing, particularly in the depth range of 200 to 1600 μm of the injection-molded bars. This result is contradictory with that reported by Zhu et al.,[18] who indicated that the degree of the overall orientation of injection-molded iPP was remarkably increased with increasing of nucleating agent. Since the material used in Zhu's work was different from ours, the

TABLE I
Crystallization Temperature (T_c) and Melting Enthalpy for iPP Containing Different Concentrations of DBS

Composition	T_c(°C)	ΔH_m (J/g)
Neat iPP	112	100
iPP/DBS (0.1 wt %)	128	105
iPP/DBS (0.5 wt %)	132	109

difference in the molecular weight and it's distribution between those used in Zhu's work and in ours may be responsible for the contrary results.

The morphological development in an injection-molded sample is governed by temperature and shear flow during the injection molding process. The important morphology-related parameters include temperature gradient, crystallization temperature of samples (may be influenced by nucleating agent or other component), and shear stress at the solid/melt interfaces. In general, a low crystallization energy barrier corresponds to an intense shear along the direction of thickness.[30] In this work, the morphological development is not only determined by the intricate balance between shear flow and temperature gradient but also determined by the competition between the formation of oriented crystal and isotropic spherulite due to the addition of DBS as nucleating agent. For the dynamic samples, the high degree of orientation is mainly attributed to the continuous shear stress during packing stage. For the static samples, in skin area, the strong orientation is as a result of the strong shear and high cooling rate induced during filling process, so the hot melt cools down quickly when contacting the cold mold wall; in the rest broad area, the slow cooling rate and the weakening of shear force leads to low orientation degree. The addition of nucleating agent increases the crystallization temperature, resulting in a decrease of energy barrier for crystallization (corresponding to increasing of shear) and an increased crystallization rate at a given depth as other processing conditions keeping constant. In addition, the shear force is too weak to induce the orientation of the quickly formed lamellae. Consequently, the orientation degree of the c-axis becomes weak gradually as the concentration of DBS increases, especially to be obvious at 200 μm away from the surface.

CONCLUSIONS

The combined effect of nucleating agent and shear on the formation of orientated structure was investigated in detail by examining the lamellar structure of injection-molded samples of iPP with DBS, layer by layer along the sample thickness. It was found that the DBS was an excellent nucleating agent for iPP, resulting in a significantly increase of crystallization temperature and decrease of crystal dimension. The shear force originated from DPIM could induce a high level of orientated structure efficiently along the shear flow direction of molded bar. The effect of shear flow to decrease the crystal dimension of iPP was found to precede the effect of nucleating agent. Although the addition of DBS into iPP was supposed to enhance the orientation level of iPP as cooperating with shear force, the oriented structure generated from the shear stress was at a quite high level so that the effect of nucleating agent on the formation of orientated structure was very weak in this study. For the static samples, the orientation degree of the *c*-axis decreases gradually from the skin to the core. With the increase of the DBS concentration, the orientation degree decreases at a given depth away from the most out surface of the sample. The result was different from what reported in the literature and worth further investigation.

References

1. Kobayashi K.; Nagasawa, T. J Macromol Sci (Phys) 1970, B4, 331.
2. Bushman, A. C.; McHugh, A. J. J Appl Polym Sci 1997, 64, 2165.
3. Okamoto, M.; Kubo, H.; Kotaka, T. Macromolecules 1998, 31, 4223.
4. Ulcer, Y.; Cakmak, M.; Miao, J. J. J Appl Polym Sci 1996, 60, 669.
5. Monasse, B. J Mater Sci 1995, 30, 5002.
6. Duplay, C.; Monasse, B.; Haudi, J. M. Polym Int 1999, 48, 320.
7. Wolkowitz, M. D. J Polym Sci Polym Symp 1978, 63, 365.
8. Trotignon, J. P.; Lebrun, J. L.; Verdu, J. Plast Rubber Process Appl 1982, 2, 247.
9. Zipper, P.; Janosi, A.; Geymayer, W.; Ingolic, E.; Fleischmann, E. Polym Eng Sci 1996, 36, 467.
10. Kantz, M. R.; Newman, H. D.; Stigale F. H., Jr. J Appl Polym Sci 1972, 16, 1249.
11. Mencik, Z.; Fitchmun, D. R. J Polym Sci Polym Phys Ed 1973, 11, 973.
12. Fujiyama, M.; Kimura, S. J Appl Polym Sci 1978, 22, 1225.
13. Kalay, G.; Bevis, M. J. J Polym Sci Part B: Polym Phys 1997, 35, 265.
14. Andersen, P. G.; Carr, S. H. J Mater Sci 1975, 10, 870.
15. Clark, E. S.; Spruiell, J. E. Polym Eng Sci 1976, 16, 176.
16. Masada, I.; Okihara, T.; Murakami, S.; Ohara, M.; Kawaguchi, A.; Katayama, K. J Polym Sci Part B: Polym Phys 1993, 31, 843.
17. Lovinger, A. J. J Polym Sci Polym Phys Ed 1983, 21, 97.
18. Zhu, P. W.; Tung, J.; Phillips, A.; Edward, G. Macromolecules 2006, 39, 1821.
19. Wang, Y.; Fu, Q.; Li, Q. J.; Zhang, G. J Polym Sci Part B: Polym Phys 2086 2002, 40.
20. Wang, Y.; Zou, H.; Fu, Q.; Zhang, G.; Shen, K. Z. J Appl Polym Sci 2002, 85, 236.
21. Fu, Q.; Wang, Y.; Li, Q. J.; Zhang, G. Macromol Mater Eng 2002, 287, 391.
22. Wang, Y.; Zou, H.; Fu, Q.; Zhang, G.; Shen, K. Z.; Thomann, R. Macromol Rapid Commun 2002, 23, 749.
23. Na, B.; Wang, K.; Zhao, P.; Zhang, Q.; Du, R. N.; Fu, Q.; Yu, Z. Q.; Chen, E. Polymer 2005, 46, 5258.
24. Wang, K.; Guo, M.; Zhao, D. G.; Zhang, Q.; Du, R. N.; Fu, Q.; Dong, X.; Han, C. C. Polymer 2006, 47, 8374.
25. Olley, R. H.; Bassett, D. C. Polymer 1982, 23, 1707.
26. Zhong, G. J.; Li, L. B.; Mendes, E.; Byelov, D.; Fu, Q.; Li, Z. M. Macromolecules 2006, 39, 6771.
27. Dean, D. M.; Rebenfeld, L.; Register, R. A.; Hsiao, B. S. J Mater Sci 1998, 33, 4797.
28. Samuels, R. J.; Yee, R. Y. J Polym Sci Part A-2: Polym Phys 1972, 10, 385.
29. Shinichi, Y.; Kaori, W.; Kiyoka, O.; Koji, Y.; Katsuharu, T.; Akihiko, T.; Masamichi, H. Polymer 2005, 46, 1675.
30. Viana, J. C.; Cunhua, A. M.; Billon, N. Polymer 2002, 43, 4185.